The HyperScout® product line

Ultimate hyperspectral imaging solution for nanosatellite platforms

HyperScout® is the cosine powered hyperspectral imaging solution for nano, micro and larger satellites.

The HyperScout® product line has been developed to provide the customer with a full spectral imaging solution experience, adding game-changing features to what a conventional camera provides, such as:

- a proven reliability in space for a multi-year mission.
- an extremely compact reflective telescope ensuring high optical quality in the spectral range of the Ultraviolet (UV) to the Thermal Infrared (TIR).
- very large storage capacity to enable high duty cycle even when platform storage and down-link bandwidth are important limitations.

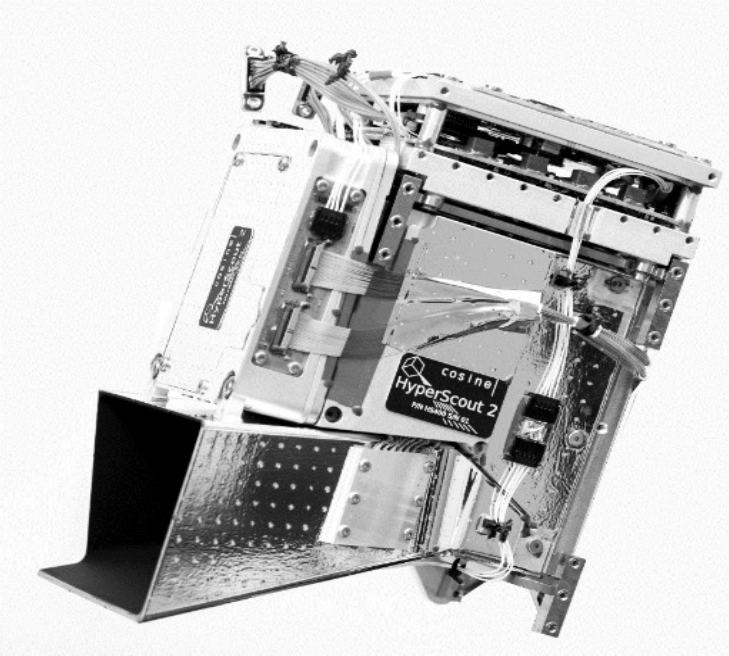

Figure 1: HyperScout® 2 Flight Model

- flexible customization of operating modes to ensure that mission constraints can be overcome efficiently, even if only known when already in orbit, without the need for lengthy design iterations on ground.
- different levels of processing and data manipulation on board to provide the most effective flexibility either by applying full processing or by selecting sub-spatial or sub-spectral regions from the data stored on the large HyperScout® mass memory unit.
- an app-like upload environment that allows the user to deploy new algorithms and run them in orbit for demonstration as well as operations.
- a deep learning tailored environment for deployment of the latest Artificial Intelligence (AI) algorithms in space.
- a ground processing tool that contains the latest machine vision techniques developed at cosine to make sure the user can process the spectral data, even when the platform attitude information contains large uncertainties, and to apply the latest radiometric and straylight correction algorithms that cosine developed for larger missions as part of the ESA Copernicus program.

HyperScout® exists in five main variants:

1. HyperScout® 1 with a VNIR hyperspectral channel (450-950 nm)
2. HyperScout® 2 with a VNIR hyperspectral channel (450-950 nm) as well as a TIR spectral channel (8-14 μm).
3. HyperScout® M with a VNIR hyperspectral channel (450-950 nm) and a volume such to fit in a

CubeSat unit

4. HyperScout® S with a VNIR hyperspectral channel (450-950 nm) offered at a medium spatial resolution of 30 m.
5. HyperScout® H for planetary exploration missions currently under development

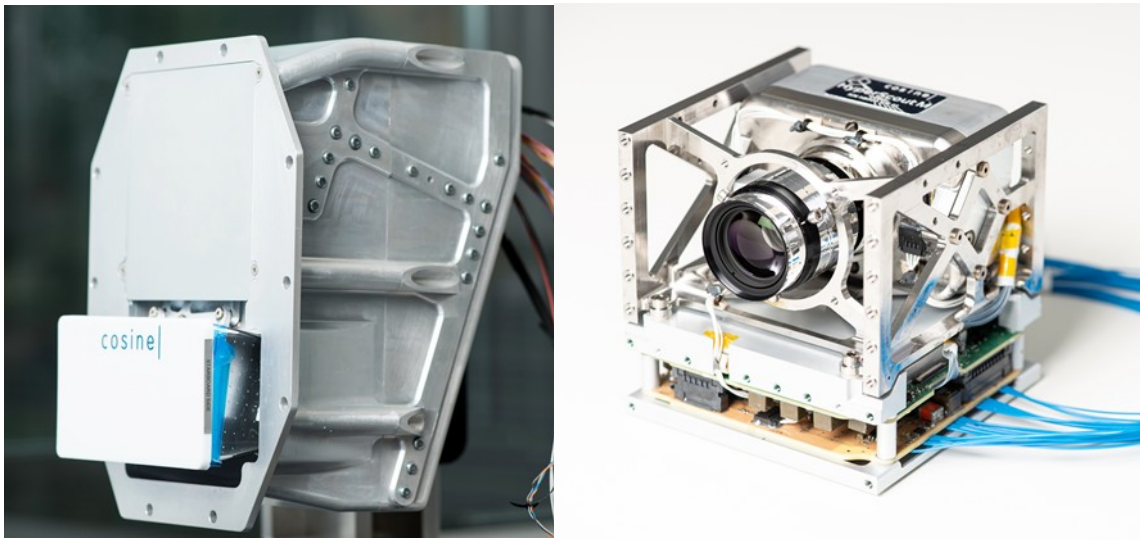

Figure 2: HyperScout® 1 engineered for interfacing onto microsatellite decks (left), and for fitting exactly a 1U CubeSat (right), also representative of HyperScout® S model providing enhanced spatial resolution.

The first HyperScout® 1 was launched in February 2018 as part of a demonstration mission with ESA TEC/MMO, and it is still operational. The first HyperScout® 2 was launched in September 2020 as part of the demonstration mission Φ-Sat-1 with ESA EOP and the Φ-lab, and it is also still operational. The list of industrial partners that contributed to both missions can be found on the cosine's website.

Additionally, a number of flight models have been delivered to customers, some of which are already in orbit. HyperScout® S offers an enhanced spatial resolution while HyperScout H is made for planetary exploration currently in development for HERA, the first ESA planetary defence mission, expected to be launched in 2024.

The HyperScout® 1 gamma includes ready solutions engineered for interfacing onto microsatellite decks (Figure 2 left), as well as a unit that fits exactly in a single CubeSat Unit (1U, Figure 2 right) named HyperScout® M, therefore suitable for satellites as small as 3U CubeSats. HyerScout® H, the solution for external deck mounting and for long interplanetary travel is expected to be available soon.

A HyperScout® 2 Flight Model is shown in Figure 1. The telescope is an athermal system based on a monolithical structure. The VNIR FPA is based on CMOS sensor and a spectral filtering element used to separate the different wavelengths.

The TIR FPA is based on a microbolometer and a multispectral filtering element. The ICU presents the contact point for HyperScout®, allowing in-flight debugging of the BEE/OBDH subsystem. Housekeeping data is logged in the idle state. It is possible to individually power down each component from the ICU.

The BEE is the latch-up protected electrical interface to the spacecraft. It distributes power, clocks, telemetry and commands between the units, controls the detector and serves as the data and control interface, providing clock timings, frame rate control, exposure and gain control. The BEE merges the data acquired with the platform ancillary information to create L0 data, which is stored in the payload Mass Memory Unit (MMU).

The OBDH serves multiple purposes, the most distinct being the platform for both the acquisition and the processing modes. During the acquisition mode, data will be transferred from the BEE into the memory of the OBDH, which is written to the MMU via SATA. If required, the OBDH can run algorithms for data processing: the data is retrieved from the MMU and processed in memory on the OBDH. Both the acquired L0 image data and processed data are stored in the payload's MMUs.

All HyperScout® models can optionally be equipped with a Vision Processing Unit (VPU) that is designed for accelerating machine vision tasks. It allows deep learning tasks such as cloud detection, radiometric processing, agricultural monitoring, hazard identification, etc. to be carried out in orbit - in real time.

HyperScout specifications

Table 1: HyperScout® specifications per model

Parameter		HyperScout 1	HyperScout 2	HyperScout M	HyperScout S
Visible Near-InfraRed Channel					
FOV [deg]		31° x 16°	31° x 16°	25° x 12°	13° x 6°
Focal length [mm]		41.25	41.25	50	100
F-number [-]		f/4	f/4	f/4	f/4
Pixel size [µm]		5.5	5.5	5.5	5.5
ACT pixels [px]		4096	4096	4096	4096
Spectral range [nm]		450-950	450-950	450-950	450-950
N spectral bands [-]		50 nominal	50 nominal	50 nominal	50 nominal
		Up to 120 in boost mode *	Up to 120 in boost mode *	Up to 120 in boost mode *	Up to 120 in boost mode *
Spectral resolution [nm]		16	16	16	16
Nominal data throughput [MB/s]		45.5	45.5	55.2	110.3
ACT GSD [m] from	500 km	67	67	55	28
	350 km	47	47	39	19
Swath ACT [km] from	500 km	280	280	225	115
	350 km	195	195	160	80
Data volume single swath [MB]	raw	2300	2300	2300	2300
	compressed	750	750	750	750
Thermal InfraRed Channel					
FOV [deg]		-	31° x 16°	-	-
Focal length [mm]		-	25.78	-	-
F-number [-]		-	F/2.5	-	-
Pixel size [µm]		-	17	-	-
Pixels size [px]		-	840 x 700	-	-
Spectral range [µm]		-	8.0 - 14.0	-	-
N spectral bands [-]		-	3	-	-
Spectral bandwidth [μm]		-	B1: 8.00 - 14.00	-	-
			B2: 10.05 - 11.24		
			B3: 11.40 - 12.50		
ACT GSD [m] from	500 km	-	330	-	-
	350 km	-	230	-	-

Parameter		HyperScout 1	HyperScout 2	HyperScout M	HyperScout S
ACT Swath [km] from	500 km	-	280	-	-
	350 km	-	195	-	-
Data volume single swath [MB]	Raw	-	250	-	-
	compressed	-	80	-	-
Physical properties					
Volume (l)		1.5	1.8	1	1.6
Mass (kg)		1.5	1.8	1.2	1.6
Peak power (W)		9	11	9	9
Hardware for data processing (including Artificial Intelligence)					
CPU		Yes			
GPU		Yes			
VPU		Yes (opt)			
Software for data processing					
VNIR onboard processing		Yes (opt)			
VNIR ground processing		Yes (opt)			
TIR onboard processing		in development			
TIR ground processing		in development			
Onboard data manipulation (ROI, pixels and frames subsampling, thumbnails, etc)		Yes (opt)			
Third party App upload		Yes (opt)			
Memories					
MMU		MMU 0: 64 GB MMU 1: 128 GB			
Interfaces					
Data		RS422			
TM/TC		RS422			
Power [V]		12 V			

* not yet validated in orbit

The VNIR hyperspectral channel

The VNIR channel is part of all HyperScout® models. The radiometric performance of the VNIR channel is illustrated in Figure 3 in comparison to a spectrally equivalent Sentinel-2 band. The Signal to Noise Ratio (SNR) ranges between 50 and 100 depending on the wavelength and on the scene.

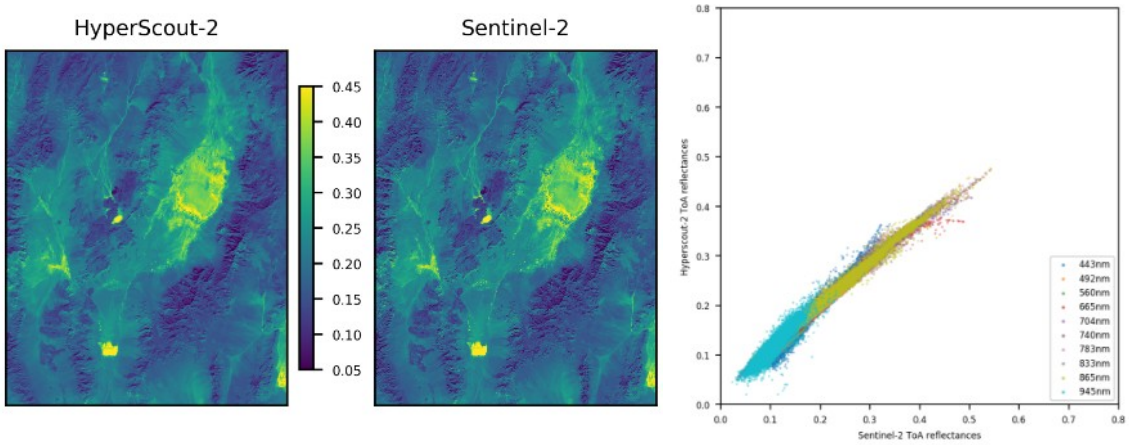

Figure 3: Comparison of top-of-atmosphere reflectance between HyperScout-2 and Sentinel-2. Left panels illustrate band images at 740 nm. The right panel shows a correlation plot between the observed S-2 reflectance and the HyperScout 2 reflectance.

The Normalized Difference Vegetation Index (NDVI) quantifies vegetation by measuring the difference between near-infrared (which vegetation reflects strongly) and red spectral reflectance (which vegetation absorbs). Figure 4 shows the NDVI, the most commonly used L2 data product in remote sensing, as derived from HyperScout® data in comparison with Sentinel-2. The mean difference in NDVI is less than 0.08 with an RMS error of 0.13.

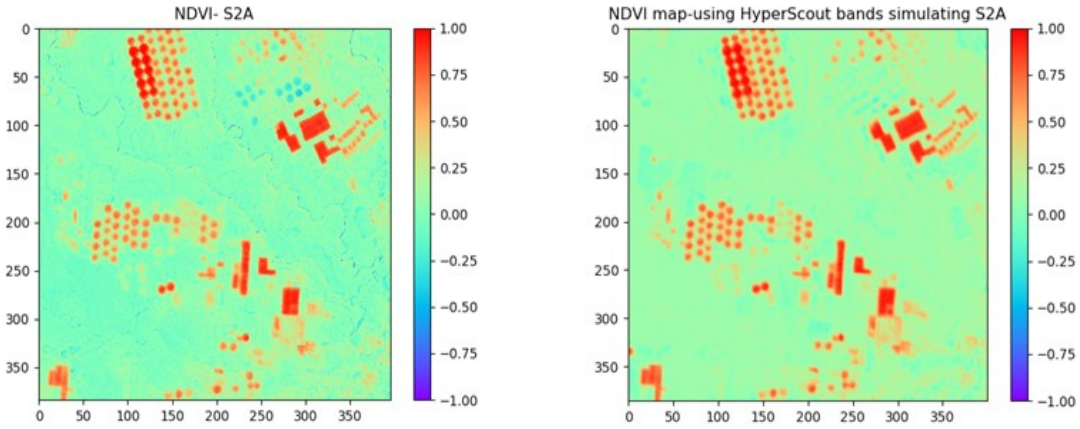

Figure 4: NDVI map using Sentinel-2A bands (left) and simulated S2A bands using HyperScout channels (fight).

Going beyond Sentinel 2

The narrow hyperspectral channels of HyperScout® make it possible to determine indices such as the Photochemical Reflectance Index (PRI), which is an important index for estimating the physiology of vegetation. The PRI is based on reflectance measurements that are sensitive to changes in carotenoid pigments (e.g. xanthophyll pigments), indicative of photosynthetic efficiency. A HyperScout PRI map is shown in Figure 5.

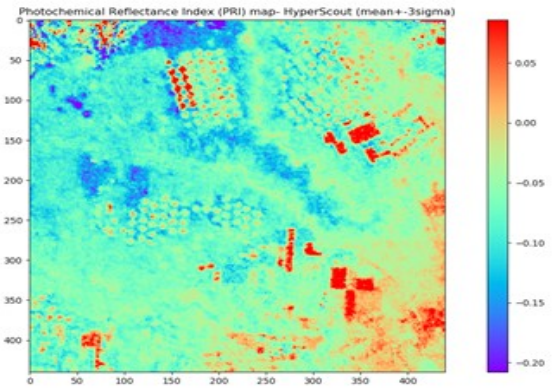

Figure 5: PRI map for the Ceylanpinar scene using a HyperScout dataset.

This information cannot be produced by Sentinel-2 and is therefore one example of complementary measurement that are not possible with existing Sentinel capabilities.

The TIR multispectral channel

The first HyperScout® 2 spectral instrument containing a multispectral TIR channel was launched into space in September 2020 for in-orbit demonstration. The in-flight operations was recently concluded and the data analysis is ongoing.

From the first assessment of the in-orbit data it is concluded that the instrument compares well with data from larger institutional satellites like Sentinel-3 and Landsat 9. Based on two acquisitions, a cold space acquisition and an acquisition over Etna Volcano (Italy), we performed a preliminarily evaluation of the radiometric performance of the TIR channel. Figure 6 shows a HyperScout 2 TIR observation, corrected for fixed-pattern noise, in comparison with the same area observed by the SLSTR sensor of Sentinel-3 and the TIRS sensor of Landsat 8.

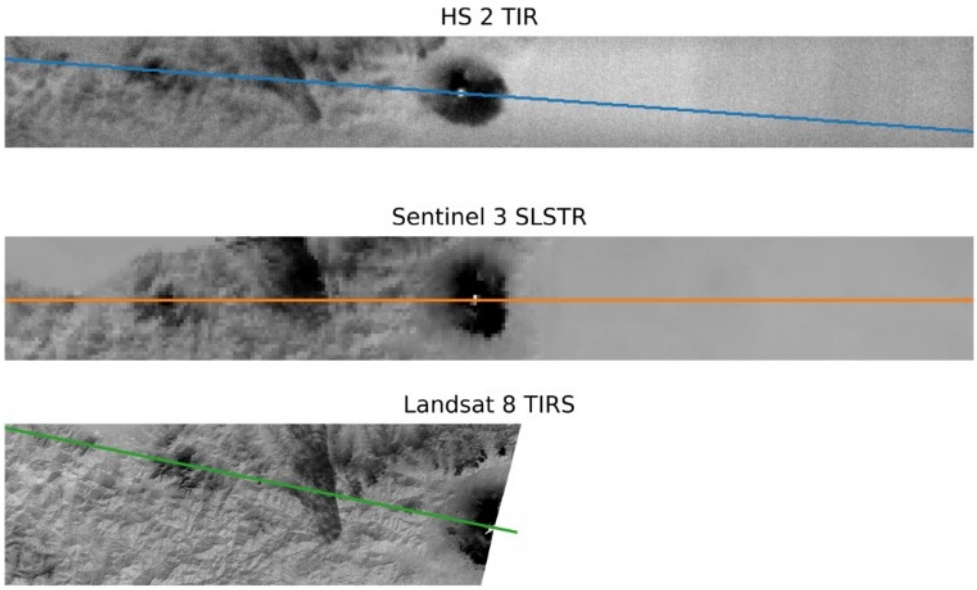

Figure 6: Brightness temperature map over Etna Volcano (Italy), as acquired by HyperScout 2 TIR, Sentinel-3 SLSTR and Landsat 8 TIRS.

Although no geometric processing was performed on the HyperScout® image, a consistency check of the radiometry was performed by comparison of a cross-section of the Sentinel-3 and Landsat 8 images and the HyperScout® 2 image at roughly the same location, as indicated by an orange line in the Sentinel-3 image, a blue line in the HyperScout® 2 image, and the green line in the Landsat 8 image. Based on tiepoints between the two images, a single offset and gain coefficient was derived. The Noise Equivalent Temperature Difference (NETD) of the HyperScout® 2 pan band is estimated to be around 1 K (Figure 1).

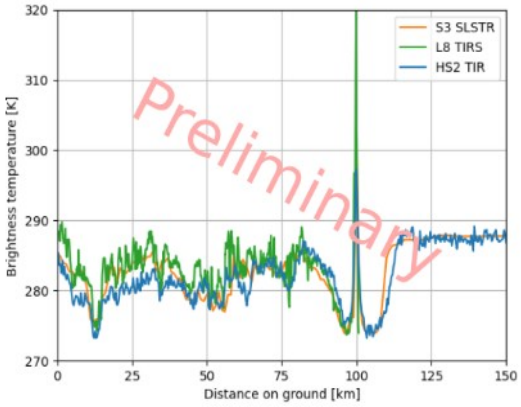

Figure 7: Comparison of a brightness temperature profile as measured by HyperScout 2 (blue), Sentinel-3 (orange) and Landsat 8 (green). Note that the two tracks are not perfectly co-registered.

On-ground processing

Using in-house developed, patent protected, computer vision techniques, the HyperScout® VNIR raw frames are stacked in spatial-spectral space as shown in Figure 9. From these remapped frames, hyperspectral cubes are formed. Using reference imagery (e.g. Sentinel-2 or Landsat-8), the cubes are reprojected into an absolute coordinate system - again using patented computer vision techniques.

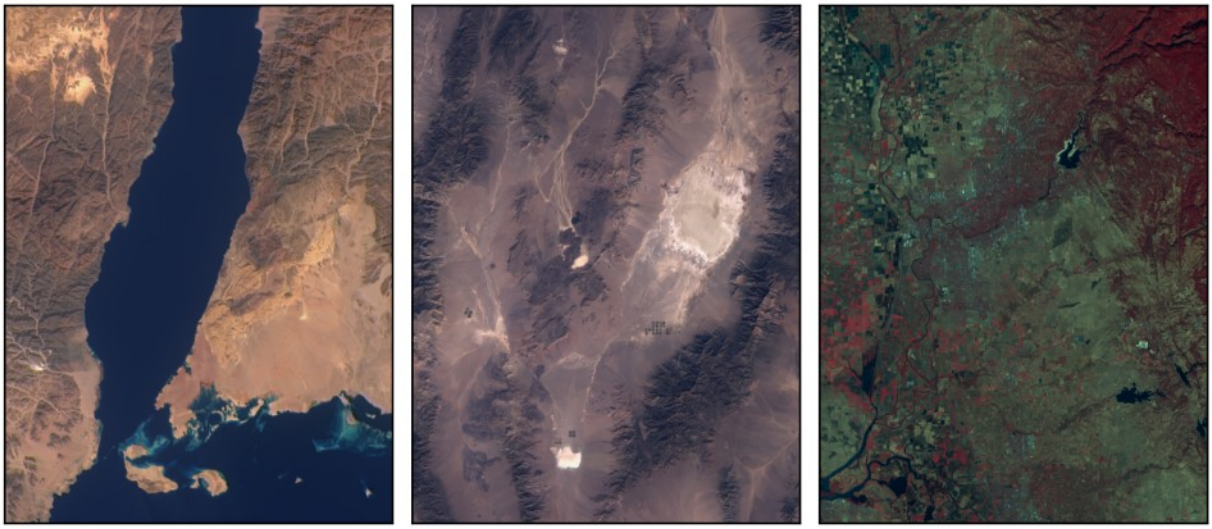

Figure 8: Left: Gulf of Aqaba [R660nm, G560nm, B480nm] Middle: Railroad Valley, Nevada [R660nm, G560nm, B480nm] Right: Moffet Field [R840nm, G660nm, B560nm]

Compared to traditional processing methods, which rely on platform dependent Attitude Determination and Control System (ADCS) data, our method is platform independent, relying solely on VNIR data itself. Because of this, HyperScout® satellites can readily be deployed on any platform without having to develop unique processing chains.

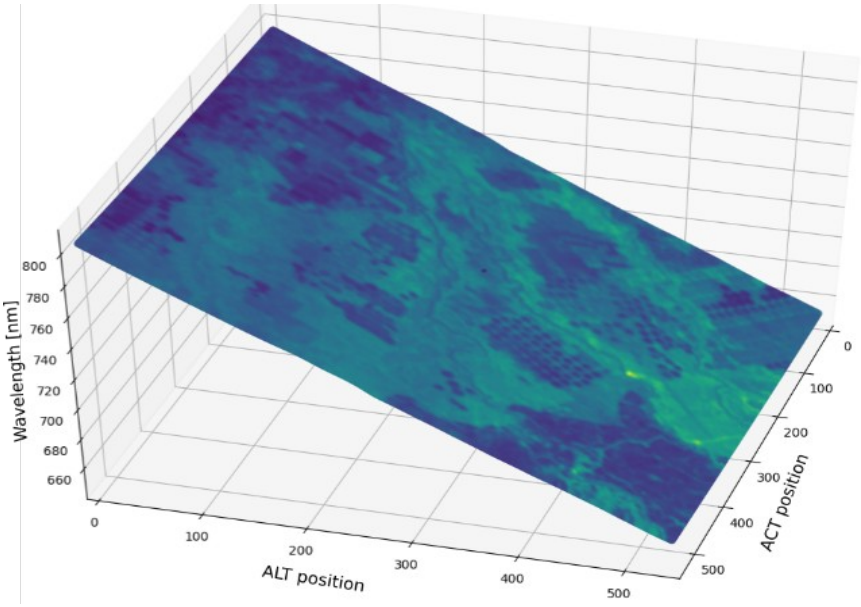

Figure 9: A HyperScout frame project in a spatial (ALT/ACT position) spectral (wavelength) space.

Performance

Example false color images composed of HyperScout® bands are shown in Figure 8. From comparison with Sentinel-2 images, a total radiometric uncertainty of the reflectance values in the order of 10% is observed, with an average absolute accuracy of the order of 5% after vicarious calibration procedures are performed. The mean geometric accuracy, as determined through tiepoint comparison with Sentinel-2, is estimated at the order of a single pixel for the current processing chain.

On-board processing

The vast majority of the previously described on-ground processing chain can also be executed in flight with the exception of the georeferencing portion because of the huge amount of storage required to store a global collection of reference imagery. Because of this, the radiometric accuracy in orbit is similar to that on ground. Although the products are not georeferenced, the interband accuracy of the data cubes is comparable to those produced with the on-ground chain.

Artificial Intelligence

With the large processing capability of HyperScout®, the user can develop and run Artificial Intelligence algorithms on board the HyperScout® product line, either on the CPU-based OBDH, or optionally HyperScout® can mount an Intel® Myriad 2 Vision Processing Unit (VPU), a System on Chip (SoC) with integrated DRAM that has been designed from the ground up, providing high-performance edge computing for vision applications. It is a heterogeneous 14-core SoC, with 2 RISC-V LEON processors managing functionality and controlling the 12 integrated vector processors.

As part of the in-orbit demonstration of HyperScout® 2, cosine and partners ran a full program, dubbed Φ-Sat-1, whose main objective was to demonstrate the in-flight ability of Deep Neural Network (DNN) inference running on the Myriad. Specifically, using a customized neural network architecture, pixels containing clouds are identified and excluded from downlinking, resulting in considerably reduced transfer volumes. This is the first time a DNN was executed in space, which paves the way for future AI experiments and applications.

An example of the output is shown in Figure 10. The solution demonstrates a pixel-to-pixel accuracy of 88.4%. The Φ-Sat-1 mission represents the first AI on-board demonstrator able to autonomously select non-cloudy images for transmission to ground. Thanks to its in-flight measured performance, Φ-Sat-1 has demonstrated the capability of AI to perform reliable and accurate on-board image processing. This technological advancement in the field of space AI, and the use of low-power COTS hardware-accelerated inference, paves the way for the exploitation of on-board AI in future EO and remote sensing applications, enabling the development of smarter and more efficient satellites for Earth Observation.

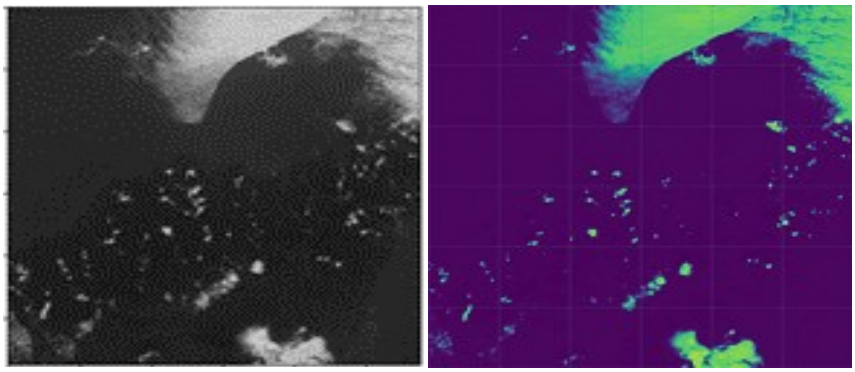

Figure 10: Original clouded image (left) and the cloud identification by the on-board neural network (right).

Besides cloud detection on board, hyperspectral AI enables a plethora of applications such as hazard detection (e.g. forest fire, flood or landslide detection), crop monitoring, chemical identification or resource monitoring, to give a few examples. Furthermore, artificial intelligence can be utilized to improve the radiometric, geometric and spectral quality beyond what would normally be possible with conventional processing techniques, as was demonstrated through the ESA/cosine MATCH project.

Sales contact:

Dr Marco Esposito

m.esposito@cosine.nl

cosine Remote Sensing BV

Warmonderweg 14, 2171 AH Sassenheim, The Netherlands

Tel. +31 71 528 4962

info@cosine.nl

remotesensing@cosine.nl

VAT NL8602.06.038.B01

Reg. NL 75245493